RSC Advances

PAPER

View Article Online
View Journal | View Issue



Cite this: *RSC Adv.*, 2026, **16**, 21099

# A novel electrochemical separation process using a polypropylene-supported membrane for simultaneous removal of nickel and manganese

Fatin A. Alnasrawi,[a] Sabreen L. Kareem[b] and Maad A. Hussein *[c]

This study explores the implementation of an electromembrane extraction (EME) system to remove heavy metals (nickel and manganese) from aqueous solutions. Using a unique electrochemical cell design with a graphite anode, a stainless-steel cathode, and a supported liquid membrane (SLM), this study examines the effect of several factors, such as carrier choice (DEHP or TEHP), applied voltage (30–60 V), pH (3–8), and metal concentration (5–30 mg $L^{-1}$), on the removal efficiency of each metal. Results show that the DEHP carrier achieved higher extraction efficiency than TEHP under all operating conditions. The applied voltage significantly enhanced the removal efficiency of each metal using the membrane. The optimal operating conditions were a voltage of 60 V, an initial pH of 6, an initial metal concentration of 15 mg $L^{-1}$, and an extraction time of 5 hours. Remarkably, under these optimized conditions, impressive removal efficiencies were achieved for each heavy metal: 84% for Ni and 71% for Mn. The FESEM and AFM results of the membrane showed a relatively homogeneous surface structure with clear porosity and low roughness, indicating the integrity of the membrane and that it is not affected by the initial treatment. After the immersion of the membrane in the DEHP carrier, a marked change in the topography of its surface was observed in the form of increased roughness and partial fullness of pores, confirming the successful fixation of the carrier and the effectiveness of the membrane in the extraction process. The results confirm that the EME technique using the SLM is an effective way to extract heavy metals from water within the optimum mentioned operational condition.

Received 4th March 2026
Accepted 3rd April 2026

DOI: 10.1039/d6ra01873d

rsc.li/rsc-advances



## 1. Introduction

Nickel and manganese are two heavy metals that are extensively used in various industries, such as in stainless steel, corrosion-resistant alloys, batteries, and metal plating.[1–3] $Mn^{2+}$ and $Ni^{2+}$ ions, commonly referred to as Mn(II) and Ni(II), respectively, are present in the wastewater of these industries and lead to serious environmental pollution. These metals are harmful when they accumulate in connective tissues without being absorbed by the body.[4,5] Heavy metals may be absorbed by humans through food, drink, air, or skin. Industrial exposure is a common method through which adults are exposed to heavy metals. Ingestion is the most common exposure route in children.[6]

Different techniques have been utilized to remove heavy metals from different effluents, such as reverse osmosis, adsorption,[7–11] membrane separation processes,[12–14] photocatalysis,[15] ion exchange, electrodialysis, and electrochemical techniques.[16] Some of these methods have proved to be effective in removing of heavy metals, yet they have no capability to retrieve the worth heavy metals that can be reused one more time. For example, a large amount of precipitated sludge is produced in the chemical precipitation method, which requires further processing. Due to high material requirements and operating costs, reverse osmosis and ion exchange methods have limited applications.[5,17]

In recent times, the supported liquid membrane (SLM) process has received increased attention from the scientific community for the separation of heavy metals.[18,19] Parhi and Sarangi separated copper, zinc, cobalt, and nickel with the help of different carriers such as LIX 841, TOPS-99, and Cyanex 272.[20] Duan *et al.* used a new sandwich-type SLM (*i.e.*, two-membrane three-compartment cell) to separate copper, nickel, and cobalt from their ammoniacal solution. They used $H_2SO_4$ as a stripping solution in two stripping compartments with different concentrations and Acorga M5640 in kerosene as a liquid membrane.[21] Ma *et al.* selectively separated copper and nickel ions from calcium ions. They used the two-stage emulsion liquid membrane (ELM) process to selectively separate copper and nickel ions. They used the Cyanex 301 carrier with LIX984N as a solvent.[22] Sulaiman *et al.* removed nickel from industrial wastewater using an SLM. Their nickel removal study was

[a]*Civil Engineering Department, College of Engineering, Kerbala University, Karbala, Iraq. E-mail: fatinen35@uokerbala.edu.iq*
[b]*Civil Engineering Department, College of Engineering, Al-Qasim Green University, Babylon 51013, Iraq. E-mail: sabreenl.kareem@wrec.uoqasim.edu.iq*
[c]*College of Engineering, Al-Karkh University of Science, Baghdad 10081, Iraq. E-mail: altaaimaad@yahoo.com; maad@kus.edu.iq*

performed using D2EHPA, octanol, and kerosene as the carrier, synergist and diluent, respectively.[23]

The application of the SLM has increased rapidly, specifically in the combination of microextraction and extraction by membrane processes, which have assisted in the development of modern methods for producing clean samples with minimal volumes of organic liquids.[24,25] Low costs, automatic operation, and the ability to operate using small samples are the additional advantages of the process.[26] The SLM, which serves as a splitting phase between the feed and acceptor phases, is made from a layer of an inert material (polymeric sheet) that is commonly filled with an organic liquid (typically dissolved chemicals).[27,28]

SLM is a non-diffusing liquid membrane type, in which the membrane phase (polymeric sheet) has an inactive position in the extraction procedure, but only works as a support layer through very microporous hydrophobic polymers that are injected with the organic solvent and made a supportive assembly for it.[29] Some of the common materials used in the SLM are polysulphones, polytetrafluoroethylene, and polypropylene. The solution flow ranges between 0.1 and 10 μm and allows the film material to accomplish an ideal stability, which is supported by these polymer films. Sometimes, a composite film is utilized, which is bonded to a rough material or one of the polymers. Polypropylene is commonly used as the material for this purpose.[30]

EME is a model of a separation technique that requires little organic solvent, which is estimated at a capacity of a few microliters, from which a small sample size is formulated. The solvent is either a supported (SLM)- or free (FLM)-type liquid membrane.[31] The key component of the EME system is the SLM, a layer of hollow, porous polypropylene fibers that retains the organic solvent and is secured within the system. The charged target analyte is isolated from the aqueous sample solution by the SLM, which is situated in a sample tank placed on a stirrer and connected to the wand stage located in a cavity of the hollow fiber. Two electrodes forming the electric field (cathode and anode) are fixed in the donor and receiver chambers, with each linked to an electrical power supply. The electrical potential difference applied between the anode and cathode causes the migration of charged ions between the two solutions.[22,32] When using the EME system to extract positively charged materials, the cathode is fixed in the recipient chamber.

This work investigates the simultaneous extraction of nickel and manganese ions from aqueous solutions to explore the feasibility of selectively extracting heavy metals from aqueous solutions using an electrically powered liquid membrane (EME) system with cost-effective electrodes. The objectives include optimizing operational parameters for maximizing extraction efficiency and understanding the behavior of four coexisting elements in the same solution under optimal conditions.

# 2. Materials and methods

## 2.1. Materials and apparatus

Nickel nitrate hexahydrate [$Ni(NO_3)_2 \cdot 6H_2O$] and manganese nitrate hexahydrate [$Mn(NO_3)_2 \cdot 6H_2O$, purity = 95%] were purchased from Central Thomas Baker (Mumbai, India). The carriers, di(2-ethylhexyl)phthalate (DEHP) and tris(2-ethylhexyl) phosphate (TEHP), were obtained from Shanghai Macklin Biochemical (Shanghai, China). The diluents, *n*-heptane, sodium hydroxide (NaOH), and hydrochloric acid (HCl), were obtained from Sigma-Aldrich (Merck, Germany).

A sensitive digital balance (4 digits), zxll3l33k, was obtained from ADAM, Japan, and a hot-plate magnetic stirrer (maximum speed = 1500 rpm), Heidolph MR Hei-Standard, was obtained from Heidolph, Germany. The ammeter was 0–0.2 A UNI-T (Kowloon, Hong Kong), and the DC power supply (0–60 V) was obtained from UNI-T, UTP3000 (Hong Kong). The magnetic stirrer with a maximum speed of 1000 rpm was obtained from Metrohm AG Herisau (Type: 18490010, Switzerland).

## 2.2. Electromembrane design

The electromembrane extraction cell, as shown in Fig. 1, was composed of two chambers with the same design and volume (385 $cm^3$). The first chamber was cylindrical and contained the donor phase. Its dimensions are: diameter of 7 cm and length of 10 cm provided from its lateral side with a cylindrical horizontal channel having dimensions (diameter of 5 cm, length of 6 cm) located above the base of the donor chamber by 2 cm. The second chamber had the same design as the first chamber and contained the acceptor phase. Each chamber was provided with a Teflon cover.[33] The cover had two holes: the first for fixing the electrode, and the second to feed the solution. A graphite plate (length = 5 cm, width = 3 cm, and thickness = 5 mm) was employed as the anode. The graphite was chosen to facilitate the anodic oxidation of water.

The cathode was a stainless-steel 316-L plate with the following measurements: a length of 5 cm, a width of 3 cm, and a thickness of 2 mm. This is the first time to use these electrodes in EME system, which makes the cost of cell fabrication cheaper than that required in the case of using platinum electrodes. A polypropylene membrane sheet with a circular configuration and an active surface area of 10 $cm^2$ was first impregnated with 1-octanol and a suitable carrier for 20 min. Then, it was placed between the channels of the two chambers and fixed using two

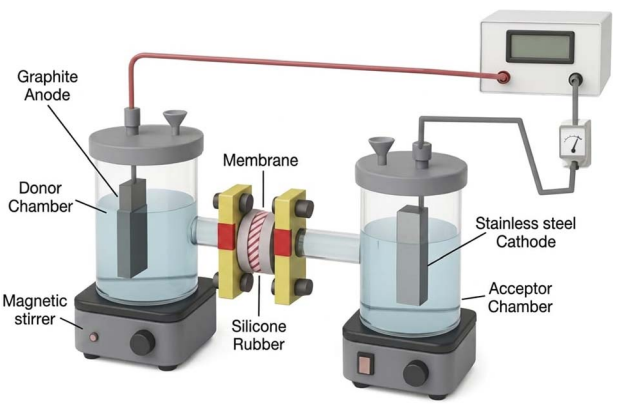


Fig. 1 Electrochemical cell containing a graphite anode and stainless-steel cathode with a supported membrane between them to remove heavy metal pollutants.

air-tight cups (each one surrounding one channel) and provided with four screws and nets. Before assembling the membrane with the channels of the two chambers, the edge of each channel was covered with RTV silicone rubber to prevent leakage. Two magnetic bars were placed in the acceptor and donor chambers to ensure constant stirring and good mixing of the solution.

### 2.3. Experimental procedure

Nickel(II) nitrate hexahydrate [$Ni(NO_3)_2 \cdot 6H_2O$] and manganese nitrate hexahydrate [$Mn(NO_3)_2 \cdot 6H_2O$] salts were used to prepare standard nickel and manganese solutions at a 1000 mg $L^{-1}$ concentration. In 1 L of distilled water, 3.8021 g of this salt was dissolved. By mixing 8.53 mL of concentrated HCl with 1000 mL of distilled water, a stock solution of the acceptor was prepared. An impregnated (membrane) solution was prepared with 100 ml by dissolving (1 ml) of each carrier in (100 ml) of 1-octanol.

The membrane was soaked in the impregnation solution for 15 min at a rotation speed of 150 rpm. Next, the two chambers of the cell were assembled and prepared for operation. Then, 100 mL of the donor phase at the required concentration of heavy metals was adjusted to the required pH by the addition of 1 M HCl or NaOH and placed in the donor chamber. 100 mL of the acceptor phase was added to the acceptor chamber. The two electrodes (graphite and stainless steel) were inserted in each chamber, and the two chambers were placed on the respective magnetic stirrers set to a rotation speed of 1000 rpm. The electrodes were connected to the power supply, and the required applied voltage was applied to the cells. Each run was started by measuring the current value during the operation and the pH of the donor and acceptor.

Due to the probability of interference from the SLM solvent, which could leak into the acceptor or donor phase, and the absorption of heavy metal ions during atomic absorption measurements, the acceptor and donor solutions were collected separately in glass vials at the end of each run, and then, they were heated until all aqueous solution had evaporated.[33] Then, these vials were refilled with deionized water, and then, the samples were taken for identification by atomic absorption spectroscopy (AAS).

### 2.4. Operating process

The operating process includes the investigation of the effects of various factors on the efficiency of heavy metal extraction using the EME technique. These factors include the voltage difference (30–60 V), donor phase pH (3–8), extraction time (1–8 hours), type of carrier (DEHP and TEHP), and initial concentration of heavy metals in the liquid phase (5–30 mg $L^{-1}$). The impact of these variables was individually analyzed to comprehend how they enhanced the removal efficiency, sensitivity, and overall effectiveness of this technique in extracting heavy metals. It is anticipated that the outcomes of this study will contribute to a better understanding of the electromembrane extraction process, ultimately enhancing the efficacy of this technique in the analysis of heavy metals in aqueous solutions.

## 3. Material characterization

### 3.1. SEM analysis

The EME-SLM, as shown in Fig. 2a, has a relatively smooth fiber surface and is free of structural defects, such as beads, with a high porosity that gives the membrane a very high surface-to-volume ratio. The pore size distribution is homogeneous, with diameters often ranging between 200 and 500 nm, ensuring stability in mechanical performance and uniformity in charge distribution when an electric field is applied. This open porosity is dynamic for ion transfer, as it delivers a high surface area that later accommodates the carrier. The lack of agglomeration is attributed to the efficiency of the electrospinning process and the stability of the polymeric solution used. Measurements (*e.g.* 378 nm and 447 nm) indicate a homogeneous distribution of the fiber diameter.[34]

After immersion in the DEHP carrier, the EME-SLM displays a fundamental morphological change, with fibers appearing "thicker" (swollen) and a thin membrane enveloping the fibers, which partially fills the interstitial spaces, as shown in Fig. 2b. This shift agrees with the successful physical fixation of the

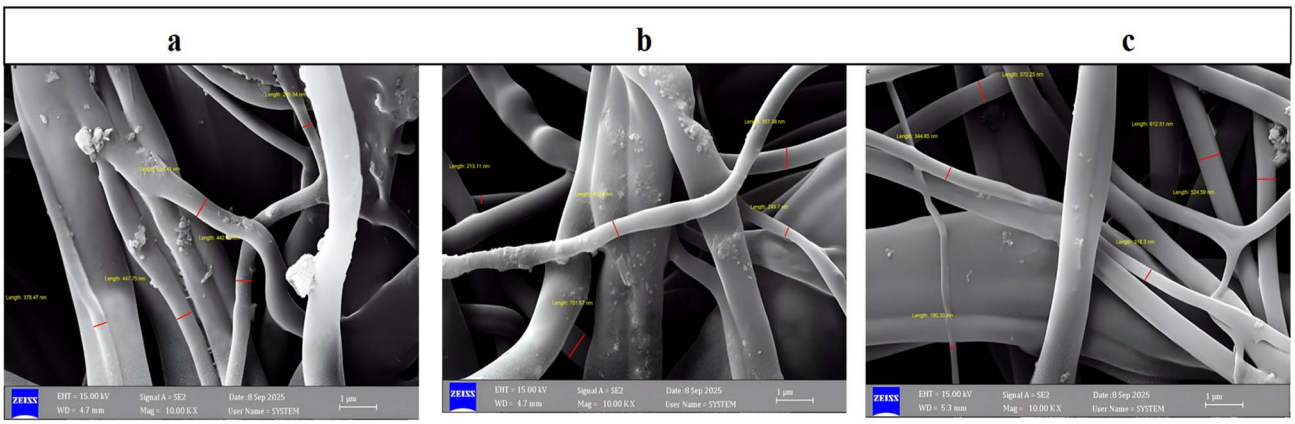


Fig. 2 FESEM images of the EME-SLM (a) before immersion in DEHP, (b) after immersion in DEHP, and (c) after $Mn^{2+}$ and $Ni^{2+}$ extraction.

organic carrier (di(2-ethylhexyl)phthalate (DEHP)) within the pores and on the surface of the fibers. The practical increase in the fiber diameter (reaching values such as 701 nm) is due to the "swelling effect" and interconnectedness. The existence of fine granules on the surface indicates distributed DEHP molecules, creating a "supported liquid membrane (SLM)". This homogeneous distribution reduces mass transfer resistance during the extraction process. Here, DEHP acts as a "supported liquid

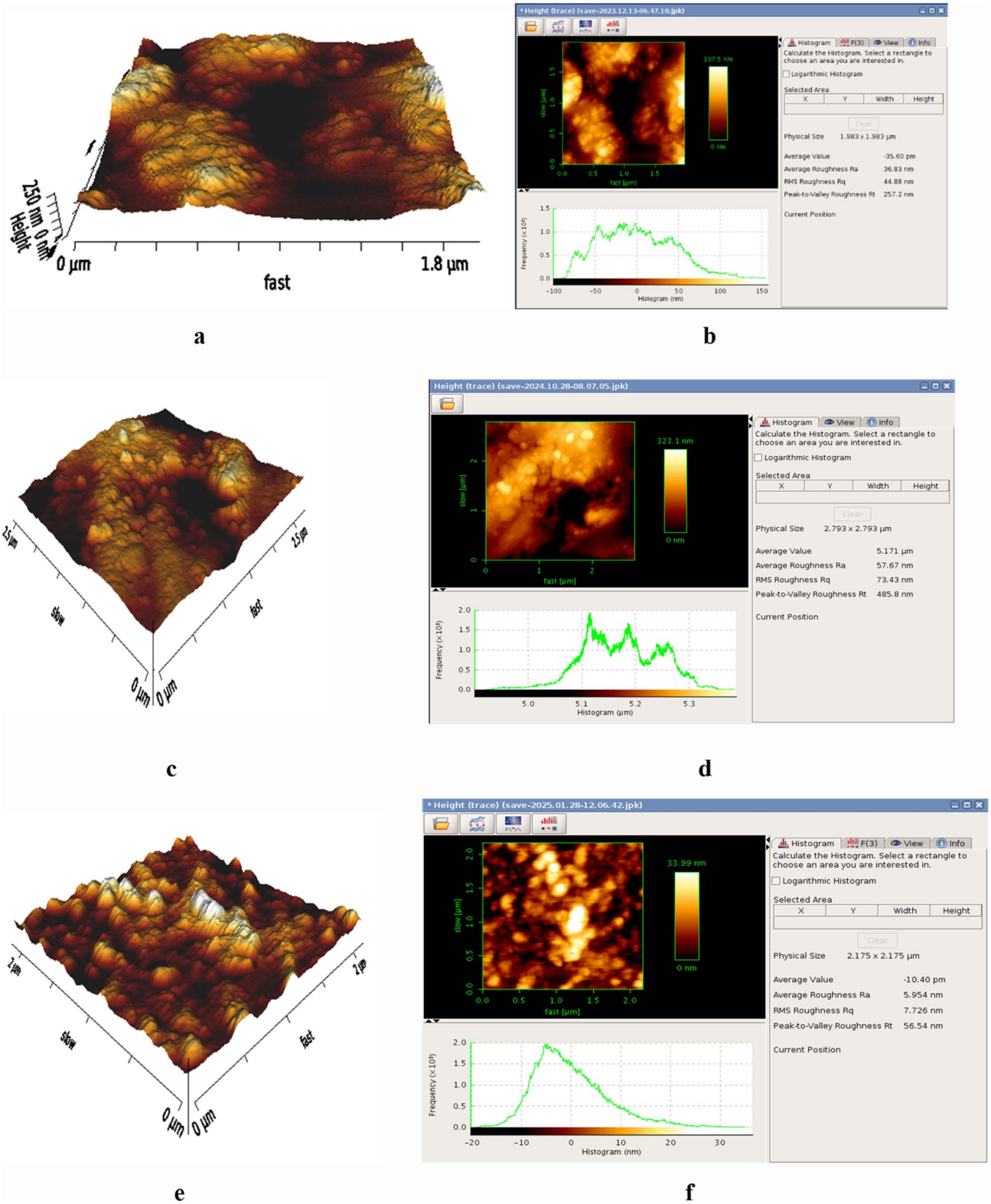


Fig. 3 AFM analysis of EME-SLM (a and b) before immersion in DEHP, (c and d) after immersion in DEHP, and (e and f) after $Mn^{2+}$ and $Ni^{2+}$ extraction.

phase". The presence of fine grains and aggregates on the surface suggests that the organic carrier has not only entered the fibers but also formed an ultra-thin film that envelops the outer surface. This morphological shift is essential to the transport process, as DEHP acts as a "shuttle carrier" that helps the dissolution and transport of metal ions from the aqueous phase to the membrane phase.[35]

Fig. 2c shows the membrane after the extraction of manganese ($Mn^{2+}$) and nickel ($Ni^{2+}$). The image shows fibers with a rougher terrain (increased surface roughness), along with the appearance of fine aggregates or "knots" along the fibers. The change in the surface texture is due to the occurrence of ion exchange and complexation between heavy metal ions ($Mn^{2+}$ and $Ni^{2+}$) and the active groups of the carrier. The retention of the fibrous structure after extraction indicates the chemical and mechanical stability of the membrane in the aqueous medium. The observed variation in measurements (180 to 612 nm) indicates the presence of active reaction regions, where the accumulation of extracted ions alters the optical and electronic properties of the fibre surface under the electron microscope beam.[36,37]

### 3.2. AFM analysis

Fig. 3a presents the AFM analysis of the EME membrane before immersion in the DEHP carrier. The results indicate a sophisticated nanomorphological structure characterized by random granular growth and irregularly sized agglomerations. The color variation in the topological map expresses the vertical elevations of the surface; the dark (brown) colors represent valleys or low-lying areas, while the light colors (yellow and white) indicate the peaks and ridges with a maximum height of 197.5 nm.[38]

As shown in Fig. 3b, the recorded roughness values reflect the nature and reactivity of the surface, with an average roughness ($R_a$) value of about 36.83 nm. In comparison, the root of the mean squares ($R_q$) value is 44.88 nm, and this tolerance ($R_q > R_a$) confirms the presence of sharp contrasts and an asymmetrical terrain rather than a smooth gradient, increasing the effective surface area of the membrane. The "top-to-bottom" roughness ($R_t$) value of 257.2 nm also shows the extent of the total variation in the terrain, which is explained by the histogram, which shows a wide distribution of heights, mostly between −50 and +50 nm, indicating a membrane with nanoporosity and high roughness that contributes to improving the physical and chemical properties for the target applications.[39]

The prepared EME membrane has a heterogeneous surface and a relatively high roughness. This type of surface is ideal if the membrane is intended for the removal of ions from the aqueous solution because the roughness increases the number of "active sites" on the surface. On the other hand, if a soft optical membrane is required, these values indicate the need to optimize sedimentation conditions to reduce the size and aggregation of the granules.[40]

The AFM analysis of the EME-SLM after immersion in the DEHP carrier is shown in Fig. 3c and d. Lighter regions (Fig. 3c) (yellow and white) indicate the membrane's "peaks" or elevated areas. In the EME membrane, these spots correspond to polymeric material aggregates or surface ridges formed by bulging when saturated with the carrier. Darker areas (brown and black) denote "valleys" or deep pores, serving as channels where the DEHP carrier is concentrated. These gaps protect the liquid carrier and act as reservoirs for ion exchange. In Fig. 3d, the data panel shows specific surface metrics: an average roughness ($R_a$) of 57.67 nm, suggesting moderate nanoroughness that enhances the surface area; an RMS roughness ($R_q$) of 73.43 nm, emphasizing variation and gradation in surface pores; and a roughness height ($R_t$) of 485.8 nm, indicating the presence of significant peaks and valleys, which facilitate carrier trapping and permit more carriers to inhabit within the membrane.[41] This alteration transforms the membrane from a physical barrier to a chemically active "functional membrane". The changes in roughness ($R_a$ and $R_q$) indicate improved contact area between the aqueous phase and the organic transporter within the membrane pores, which is crucial for selective transport.

DEHP acts as a carrier that binds specifically to divalent metal ions like Ni and Mn, transporting them across the membrane under an electric field through EME processes.[42] When submerged in the DEHP carrier, pore swelling occurs, permitting the carrier to enter polymeric pores and create protrusions, which are visible as bright areas in AFM images. This increases the surface roughness and contact area. Dark regions signify liquid-filled channels, functioning as "chemical elevators" that transport Ni and Mn ions owing to the electric motive force. The high chemical affinity of DEHP ensures selectivity, avoiding unwanted ions and concentrating target metals at the reception end. The stability of peaks and valleys, shown by $R_q$ and $R_t$ values, indicates the membrane's structural integrity and its long-term effectiveness in industrial and environmental demineralization applications.[43]

Fig. 3e illustrates a notable alteration in the membrane's surface topography, offering direct evidence of efficient ion exchange and transport. Bright-yellow/white peaks indicate active sites where chemical complexes are formed between the carrier and extracted mineral ions ($Ni^{2+}$/$Mn^{2+}$). Dark-brown/black valleys show the porous channels within the initial polymeric membrane. The values in Fig. 3f ($R_a = 5.954$ nm and $R_q = 7.726$ nm) are drastically lower than those in the initial image ($R_a = 57$ nm) prior to extraction, indicating the presence of a surface smoothing effect.[42] This is due to the filling of large gaps and pores with $Ni^{2+}$/$Mn^{2+}$ and associated compounds, which decreases the surface contrast. The decrease in $R_t$ from 485.8 nm to 56.54 nm reflects the stability of the thin liquid film (SLM) and the absence of cracks or bursts after ion insertion, thus improving membrane stability. The histogram reveals a symmetric distribution, which indicates uniform $Ni^{2+}$/$Mn^{2+}$ ion coverage on the membrane surface, which is important to prevent pore clogging in specific areas. The distribution confined between −20 nm and +30 nm proves that the membrane's microstructure remains intact without chemical corrosion by ions or carriers. AFM results demonstrate that the EME-SLM shows high kinetic compatibility with $Ni^{2+}$/$Mn^{2+}$ ions. The transformation from high nanocoarseness (initially aiding ion capture) to a more stable, smoother surface after extraction

shows the membrane's ability to efficiently trap heavy metals within the supported liquid structure. This morphological change reduces membrane fouling and ensures high selectivity for target metals in complex industrial wastewater, making it a sustainable and successful water resource management solution.[43]

# 4. Results and discussion

## 4.1. Selection of the extraction time

To determine the best extraction time in the liquid phase, the experiment was conducted by changing the extraction time from 1 hours to 8 hours, as shown in Fig. 4. The experiment was carried out under the conditions of an initial concentration of 10 mg $L^{-1}$, a pH of 5, and a voltage of 60 V using DEHP as a carrier. The results indicated that the concentrations of Ni and Mn gradually decreased, achieving the maximum removal effectiveness after 5 hours. After five hours, the concentrations began to rise again, indicating a decrease in the stability of the electromembrane extraction (EME) system after this time. When the optimal duration (5 hours) was reached, the concentration of each metal in the original solution began to increase again [44]. The Ni concentration increased from 4.3 mg $L^{-1}$ after 5 hours to about 6.8 mg $L^{-1}$ after 8 hours, and the $Mn^{2+}$ concentration increased from 6.0 mg $L^{-1}$ after 5 hours to about 7.6 mg $L^{-1}$ after 8 hours.

A portion of the SLM may have begun to dissolve and leach into aqueous solutions on both sides of the cell, reducing the thickness of the membrane, which affects the mass transfer and affects its ability to separate the two aqueous phases. Thus, 5 hours was shown to be the optimal duration for the extraction process, allowing for effective removal by the EME method. This predetermined duration was used in subsequent trials to evaluate other factors. Ni exhibited a greater and faster removal effectiveness than Mn. At this favourable stage, the nickel concentration decreased to about 4.3 mg $L^{-1}$, while the Mn concentration decreased to about 6.0 mg $L^{-1}$. The difference in selectivity is due to the formation of more stable or preferential complexes between the DEHP carrier and nickel ions ($Ni^{2+}$) compared to manganese ions ($Mn^{2+}$) at pH 5.

The curve displayed two overlapping phases resulting from the nature of the electrochemical system and the competition between ions. The decrease in the concentration represented the movement of metal ions from the solution through the polypropylene-supported membrane due to electrical motivation and adsorption. In binary systems, ions have varying affinities towards the active sites on the membrane. As the process continues, the ions with higher affinity, Mn, may expel the weaker-bonded ions that were initially adsorbed, causing them to be relaunched in the solution, which explains their increased concentration after reaching a temporary saturation point.[45]

## 4.2. Selection of the carrier

In this work, di(2-ethylhexyl)phthalate (DEHP) and tris(2-ethylhexyl)phosphate (TEHP) at 1% v/v were examined as carriers with 1-octanol to remove Ni and Mn from solutions. Fig. 5 illustrates the impact of the carrier type. All experiments were conducted under the conditions of initial Ni and Mn concentrations of 10 mg $L^{-1}$, a pH of 5, an extraction time of 5 hours, and a voltage of 60 V. The results show that the removal efficiency of Ni and Mn ions using the EME-SLM technique increases with time for both carriers, DEHP and TEHP, but the DEHP carrier clearly outperforms the TEHP carrier. After 5 hours, the highest efficiency recorded for Ni using DEHP and TEHP carriers is 74% and 64%, respectively. The removal of Mn is typically inadequate, with DEHP-Mn exhibiting an efficiency of 55%, whereas TEHP-Mn exhibits the lowest efficiency at 49%.[33]

DEHP is the most useful and selective carrier under these conditions due to its acidic properties (cation exchanger), which accelerate the formation of more stable complexes with Ni than with Mn at pH 5. DEHP is an organic acid extract that enables cation exchange, as it possesses an acidic hydrogen atom capable of interacting with divalent metal ions ($Ni^{2+}$ and $Mn^{2+}$) to form hydrophobic complexes that cross the membrane. Acid exchange is altered by the voltage difference (60 V) in the EME

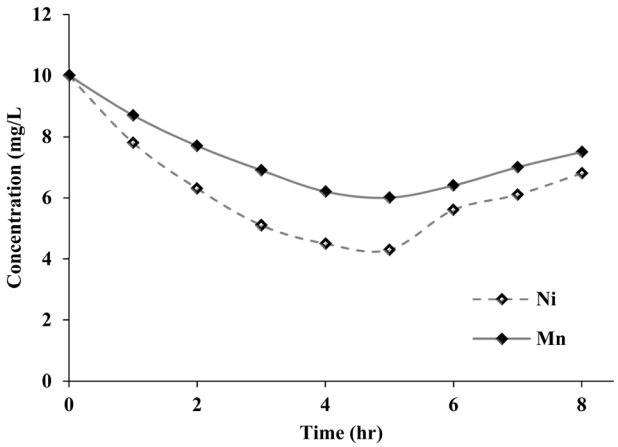


Fig. 4 Effect of the extraction time on the concentration gradient of $Mn^{2+}$ and $Ni^{2+}$ ions.

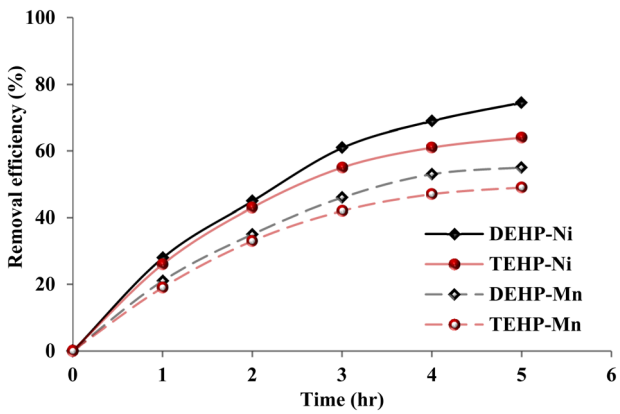


Fig. 5 Impact of the carrier type on the efficacy of removing $Mn^{2+}$ and $Ni^{2+}$ ions.

technology, which promotes ion movement. TEHP primarily acts as a neutral solvent extract, relying on synergistic or coordination reactions rather than acid ion exchange, leading to a substantial reduction in the transfer efficiency of positive metal ions under these conditions. In all cases, Ni removal is notably superior to Mn removal, with the DEHP carrier increasing the Ni removal rate of up to 74%, compared with 55% for Mn. This selectivity indicates that the DEHP transporter forms more stable complexes with $Ni^{2+}$ ions than with $Mn^{2+}$ ions at pH 5, thereby enhancing the efficiency of nickel transport across the membrane.[44]

### 4.3. Effect of the applied voltage

At an initial concentration of 10 mg $L^{-1}$ and a pH of 5 using DEHP as the carrier, five voltages varying from 30 to 60 V were tested to estimate the effect of the applied voltage on the removal efficiency of Mn and Ni using the EME-SLM system. Fig. 6 exhibits how the process voltage influences the removal of each heavy metal. The removal efficiencies of Ni and Mn increase with the voltage, peaking at 60 V. A higher electrical potential difference enhances the electrophoretic force on the positively charged complex ions formed between the metals and the DEHP carrier, improving their migration through the SLM and decreasing transfer resistance. Accordingly, Ni removal reaches approximately 75% (Fig. 6a) and Mn removal reaches around 55% (Fig. 6b) at 60 V. To overcome the transport limitations, ion transport is usually constrained by the diffusion rate across the aqueous boundary layer of the initial solvent. However, applying high electrical energy confirms that migration predominates as the transport mechanism, raising the overall flux rate across the membrane and achieving the fastest and most efficient removal from the original solution.[46]

A different pattern is observed with respect to the concentrations of Mn and Ni in the acceptor phase, as shown in Fig. 7. The acceptor concentration peak levels appear at medium voltages (40–50 V) and not at the maximum voltage. The concentration in the acceptor solution does not follow this trend, peaking at a medium voltage of 40 V, with the highest concentration of 4.8 mg $L^{-1}$ for Ni and 4.1 mg $L^{-1}$ for Mn. At the maximum voltage (60 V), the acceptor concentrations drop to 3.9 and 3.1 mg $L^{-1}$ for Ni and Mn, respectively.

This loss is attributed to the very high voltage that imposes extreme electrical and thermal stress on the thin membrane layer, potentially leading to membrane instability. This instability can cause the ions to leak or re-release from the acceptor side or even return to the donor solution. Furthermore, the membrane's instability decreases its selectivity, permitting ions that have been transported or accumulated at the membrane

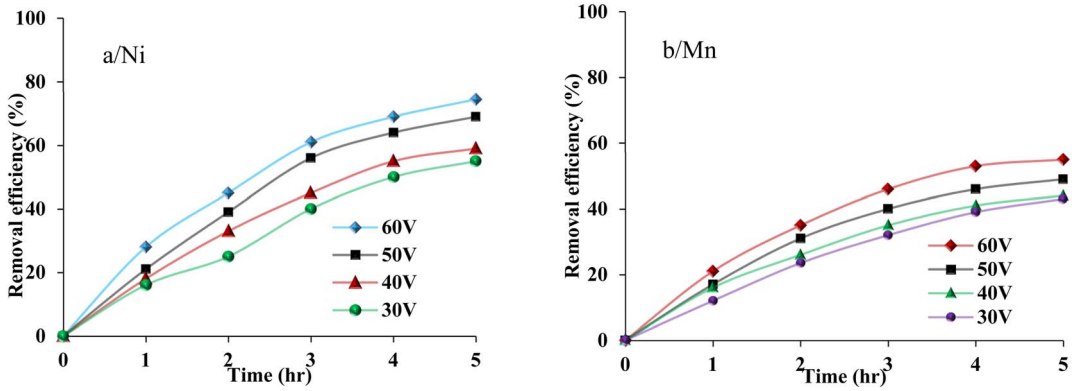


Fig. 6 Effect of the applied voltage on (a) $Ni^{2+}$ and (b) $Mn^{2+}$ removal efficiencies.

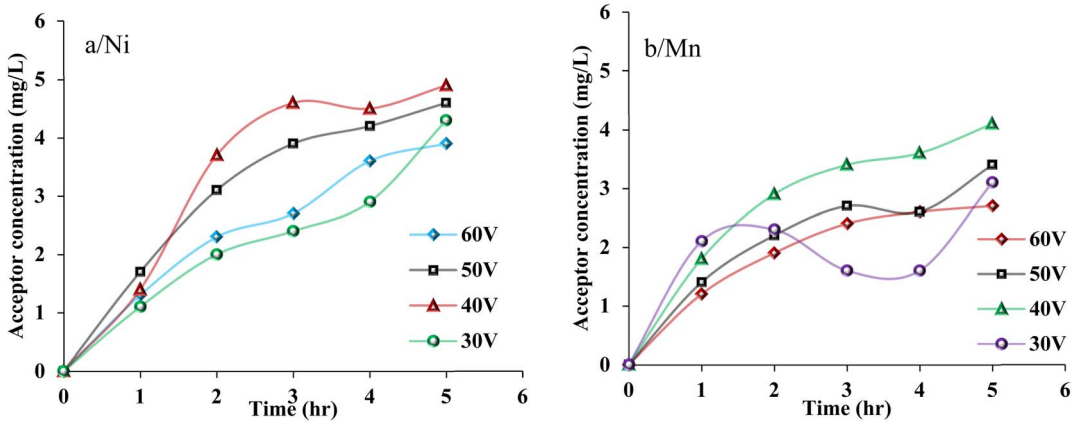


Fig. 7 Effect of the applied voltage on the concentration gradient of (a) $Ni^{2+}$ and (b) $Mn^{2+}$ ions in the acceptor.

interface to seep back into the original solution (posterior extraction). As a result, the net concentration in the receptor solution decreases, regardless of the high initial extraction rate.[46]

The results conclude that while a high voltage (60 V) is the most effective in improving the "extraction efficiency" of ions from the initial solution, a moderate voltage (40 V) improves the "aggregation efficiency" of the received solution by maintaining the stability of the membrane.[47] High voltages also lead to concentration polarization, where ions accumulate at the membrane interface because the migration rate exceeds the reverse diffusion rate. This causes increased internal resistance and limitations in mass transfer, a phenomenon demonstrated in recent studies on electrodialysis membrane systems, where an increased current and voltage density deepens the polarization layers and restricts ion transport across the membrane, thus limiting transfer efficiency.[48] Consequently, the entire flux removed from the donor phase is not converted into an equivalent net transfer in the acceptor phase. In contrast, a voltage of 40 V exhibits a better balance between the electromotive force and mass transfer efficiency, resulting in the highest net accumulation in the acceptor phase. These results suggest that there is an optimal voltage for maximizing the net transfer efficiency, rather than simply relying on the highest applied voltage.

Fig. 8 shows the relationship between the applied voltage and the electrical current flowing through the membrane in the EME-SLM system. The diagram shows a strong direct relationship between the applied voltage and the current transmitted in the electromembrane extraction (EME) system.[49] At any given moment, the use of a higher voltage results in a much higher current, which corresponds with Ohm's law. The current gradually increases as the voltage increases, reaching its highest value at 60 V (40 mA) after 5 hours, followed by 50 V (30 mA), then 40 V (26 mA), and the lowest current at 30 V (18 mA). Additionally, it has been observed that the electric current increases over time at all voltages, starting at almost zero and continuing to increase over the duration of 5 hours.[47] This increase with time can be explained by the fact that the current in the EME-SLM technology reflects the flow of charged ions through the liquid membrane. As the extraction process continues, the concentrations of moving ionic compounds (such as Ni/Mn-DEHP compounds) in the membrane may increase. This facilitates ion transport and reduces the overall resistance of the system, allowing for a higher current flow over time. This high current stimulates the migration of metal ions, which enhances the extraction efficiency.[50]

The high voltage significantly affects the pH levels of the donor and acceptor solutions. Fig. 9 shows the dynamic correlation between the applied voltage and the pH changes in both solutions for 5 hours. The mechanism of action of the DEHP carrier as a cationic exchanger occurs according to the following general reaction:[51]

$$M2 + (Donor) + 2HR\ (Membrane) \rightleftharpoons MR_2\ (Membrane) + 2H + (Donor)$$

To investigate the variation in the pH of the donor solution (pH), the pH of the donor solution starts at 5 and then drops sharply within the first hours to a range of 2.1–2.5. It then stabilizes or experiences a slight decline during the remaining period. A low pH, which indicates high acidity, occurs when the DEHP transporter exchanges a hydrogen ion ($H^+$) with a divalent metal ion ($Ni^{2+}$ or $Mn^{2+}$) at the interface with the donor solution. Each metal ion releases an extracted $H^+$ ion into the donor solution, resulting in a rapid rise in the $H^+$ concentration and a subsequent decrease in the pH. Higher voltages (60 V and 50 V) cause a greater decrease in the pH (increased acidity) than low voltages (30 V and 40 V). This is in line with the observation that higher voltages enhance the extraction efficiency, resulting in the release of more $H^+$ ions into the donor solution.[52]

The pH of the acceptor solution starts at pH 2 and rises rapidly within the first hours, reaching near 4.5–5, possibly due to the $OH^-$ ion flux or an initial deficiency of positive ions. After that, it either gradually decreases or stabilizes, except for the 60 V curve. When the pH of the membrane/acceptor solution falls in the acidic region, the metal ions in the solution are released, while the carrier material returns to its protonated state within the membrane. The acceptor solution, which is often very acidic, catalyzes the reverse reaction (precipitation/

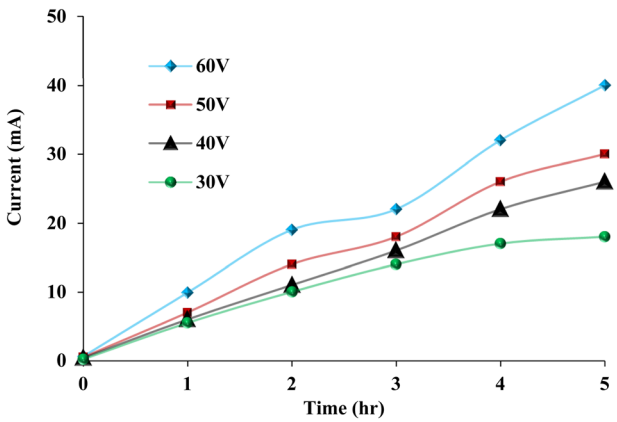


Fig. 8 Effect of the applied voltage on the current.

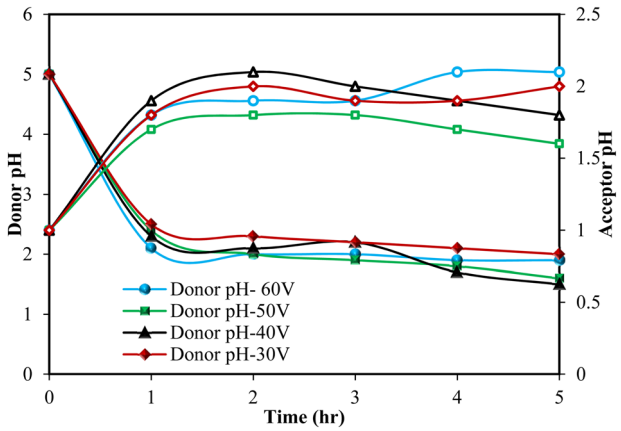


Fig. 9 Effect of the applied voltage on the pH of the donor and acceptor.

release), leading to the accumulation of metal ions. An increase in the pH at high voltages may indicate the excessive transfer of negative ions (such as hydroxide ions or residual anions) or membrane instability, which allows chemical species to overlap, leading to a decrease in the concentration of hydrogen ions. In an acceptor solvent, the movement of ions increases with the voltage, which promotes chemical changes in both phases.[49]

### 4.4. Effect of the pH

Fig. 10 shows the impact of the pH of the donor solution on the removal efficiency of Ni and Mn using the EME-SLM system. The experiment used the DEHP carrier with a preliminary concentration of 10 mg $L^{-1}$ and a voltage of 60 V for 5 hours. It has a curved pattern that reveals the balance between ionic competition and sedimentation of the metal ions. The removal efficiency of nickel depends considerably on the pH (less than 60 V, 5 hours, DEHP bus). The removal efficiency peaks at 80% at pH 6, dropping to 74% at pH 5 and 45% at pH 3. The decrease at low pH is due to the intense competition from hydrogen ions ($H^+$) for the bonding sites in the DEHP carrier. The effect of pH on manganese removal efficiency over time at different levels of pH of the donor solution is that the ideal region is the maximum manganese removal efficiency of 66% achieved at pH 6, followed by 61% at pH 7 and about 55% at pH 5. Reduced efficiency at low (acidic) pH occurs as follows: at pH 3, the efficiency declines markedly to 40%. This results from the fierce competition between hydrogen ions ($H^+$) and manganese ions ($Mn^{2+}$) for binding sites in the DEHP transporter, which restricts the formation of transport complexes.

The effect of the pH of the donor solution on the concentration of Ni and Mn ions accumulated in the acceptor solution over time under electromembrane extraction (EME) conditions is shown in Fig. 11. The highest Ni concentration in the acceptor solution reaches approximately 3.9 mg $L^{-1}$ after 5 hours at pH 5. Although the maximum Ni removal efficiency from the original solution is observed at pH 6, pH 5 provides the best net concentration in the acceptor solution. This indicates that a medium at pH 5 achieves the optimal balance between the removal of nickel from the source and the ability of the receiving solution (which is usually highly acidic) to effectively remove nickel from the DEHP transporter, ensuring the highest accumulation concentration. Conversely, the efficiency decreases sharply at the extremes. At pH 3, the concentration of nickel decreases significantly to about 2.6 mg $L^{-1}$ due to the intense competition from the high concentration of hydrogen ions ($H^+$) at the binding sites on the DEHP carrier, which delays the capture of nickel. At pH 8, the concentration rises to about 3.7 mg $L^{-1}$ due to the formation of nickel hydroxide ($Ni(OH)_2$), which begins to precipitate in the original solution, decreasing the number of the free $Ni^{2+}$ ions available for electrolysis.[53]

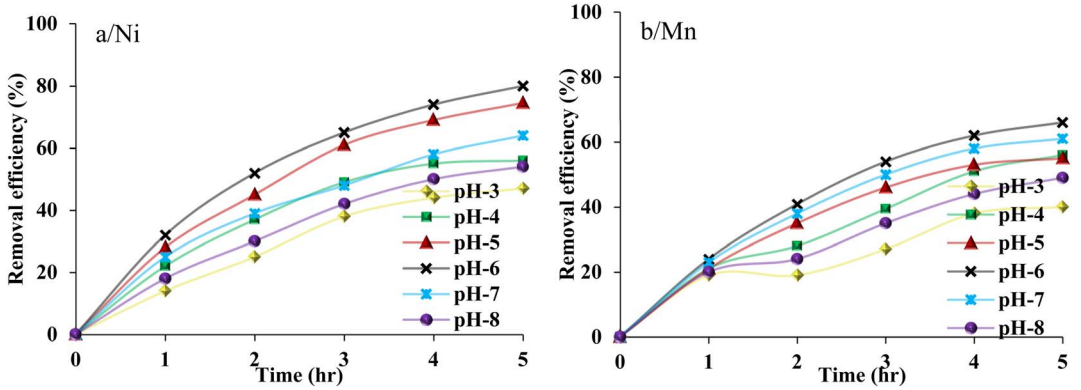


Fig. 10 Effect of the pH on (a) Ni and (b) Mn removal efficiencies.

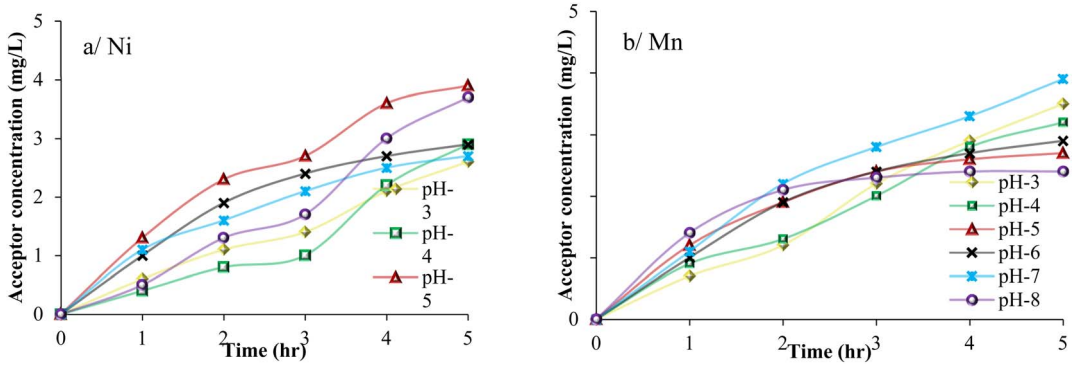


Fig. 11 Effect of the pH on (a) Ni and (b) Mn concentrations in the acceptor.

The difference in the concentration of Mn in the acceptor solution relative to the pH of the donor solution results from the interaction between the efficiency of extracting manganese from the source and the ability of the receiver solution to re-release it. According to the diagram, pH 7 is the optimal pH for manganese collection, with the concentration peaking at about 3.9 mg $L^{-1}$ after 5 hours. At pH 7, the competition from hydrogen ions ($H^+$) is minimal, which is vital for manganese ($Mn^{2+}$) due to its weak affinity for the DEHP transporter compared to that of nickel. This allows the carrier to gain and transport the maximum amount of $Mn^{2+}$ across the membrane. Despite the high pH, pH 7 remains within the range in which manganese hydroxide ($Mn(OH)_2$) is not significantly precipitated, leaving most of the ions available for extraction.[44]

The higher concentrations observed at pH 3 and pH 4, around 3.5 mg $L^{-1}$ and 3.2 mg $L^{-1}$, respectively, can be clarified by electrochemical propulsion as follows: although low pH increases the competition from $H^+$ ions in the source solution, a high $H^+$ concentration in the donor phase can aid the stripping in the strongly acidic receiving phase, maintaining relatively high concentrations there. At pH 5 and pH 6, the competition from $H^+$ remains considerable for Mn, reducing the transport efficiency. At pH 8, the concentration decreases to approximately 2.4 mg $L^{-1}$ due to Mn precipitation in the source solution. Even though pH 8 is more basic, most manganese is in the form of precipitated hydroxide, which makes it unavailable for electrodialysis and thus lowers the final concentration in the acceptor solution.[54]

The analysis of the effect of the pH on the electric current in the EME-SLM for the removal of Mn and Ni is shown in Fig. 12. The figure shows that the pH greatly influences the movement of ions, which translates directly into the measured electric current. The current is an indicator of the activity of the positively charged Mn and Ni ions being transported across the liquid membrane by the electric motive force. At pH 3, the current is 34 mA, and at pH 8, the current reaches 67 mA. This elevation indicates a significant increase in the movement of the total ions across the membrane due to an increase in the concentration of $OH^-$ in the solution or an improvement in the ionization of the extracted substance (carrier) in the liquid membrane, which generally facilitates the transfer of ions.[55] Under basic conditions, Mn and Ni ions may begin to precipitate as metal hydroxides before reaching the membrane. This deposition reduces the removal efficiency even if the current is high because the current may result from the movement of ions other than the target metals. At neutral pH (pH 6 and 7), the current shows high values (approximately 42 and 49 mA, respectively). This pH range is typically best suited for heavy metal removal. Mn and Ni ions are in their fully stable cationic (positively charged) form, making them available for binding to and transport carriers in the liquid membrane. The high current strongly binds with Mn and Ni ions for binding sites with the transport material within the membrane. This intense competition reduces the transport of Mn and Ni ions, resulting in an overall reduction in the current allocated to transporting these metals across the membrane.[56]

Fig. 13 shows the effect of the initial pH (value in the range of 3–8) in the donor solution on the pH change in both donor and acceptor solution over a 5 h period. The pH of the donor solution mainly affects the rate of transport of compounds through the liquid membrane. The pH of the donor is selected to ensure that the contaminants to be removed, Ni and Mn, are in their appropriate ionic form, which enables their effective binding to the carrier material within the liquid membrane. The positive metal ion (Mn and Ni) extraction process is often more efficient in medium-to-high pH (less acidic) environments, where there is less competition from $H^+$ ions for the binding site. If the donor solution is too acidic (low pH), the concentration of $H^+$ ions will be too high. These ions will compete strongly with metal ions to bond to the carrier. This competition reduces the amount of minerals transported to the membrane, thus reducing their concentration in the received solution.

The pH of the acceptor solution is the driving force for the release of contaminants from the liquid membrane into the clean solution. The donor determines the direction of the acidity: for extraction, the acceptor solution is designed to be highly acidic. When a liquid membrane is used, the hydrogen ions in the receiving solution break the bonds between the carrier material (which holds Ni and Mn) and metals. The carrier releases its metals into the receiving solution and then returns to the donor solution to capture more metals. The high

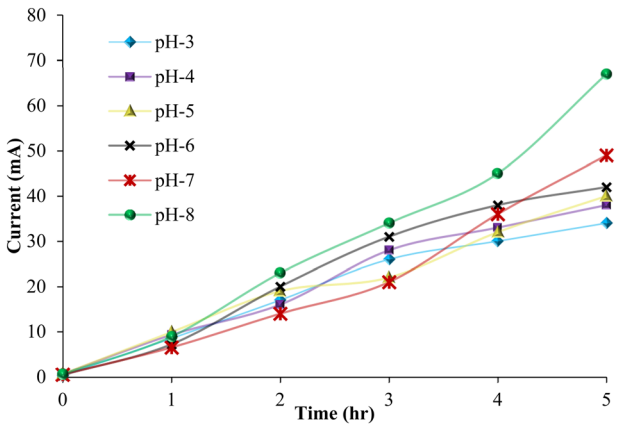


Fig. 12 Effect of the pH on the current.

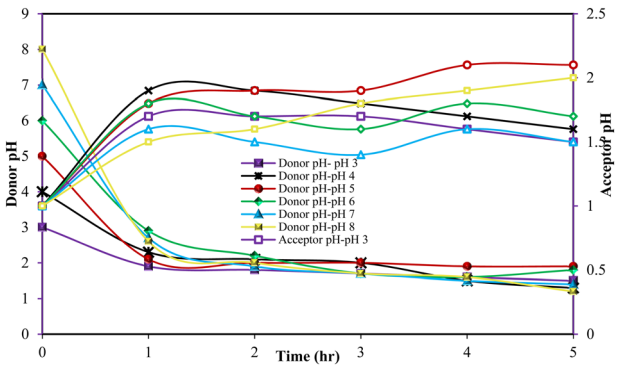


Fig. 13 The effect of initial external pH on the donor and the acceptor pHs.

concentration of hydrogen ions in the receiver "attracts" the metal ions from the membrane, ensuring that the receiving solution becomes rich in the extracted minerals. The bottom line is that the relationship between the pH of the donor and the receiver is opposite and complementary to ensure that the ions move in one direction.[19]

### 4.5. Effect of the initial Mn and Ni concentration

Fig. 14a and b show the effect of the initial concentration of Ni and Mn under optimal conditions (pH 6, 60 V, DEHP carrier, and 5 h-contact time) on the competitive removal efficiency. The removal efficiency of Ni ions reaches 84% at a 15 mg $L^{-1}$ initial concentration. This elevation indicates that the increase in the initial concentration in the low range (5 to 15 mg $L^{-1}$) significantly enhances the concentration gradient, which is the driving force for the mass transfer of Ni ions across the membrane, without the DEHP having yet reached the saturation point. Once this optimal concentration is exceeded, the removal efficiency begins to decline rapidly, reaching 62.3% at a 30 mg $L^{-1}$ initial concentration; this decrease is due to the limited saturation of the carrier in the liquid membrane. At high initial concentrations, the number of $Ni^{2+}$ ions increases significantly, but the number of carrier molecules (DEHP) in the membrane remains constant. This leads to the saturation of bonding sites, all active sites are quickly occupied, and a limited flow rate is obtained (flux).[5]

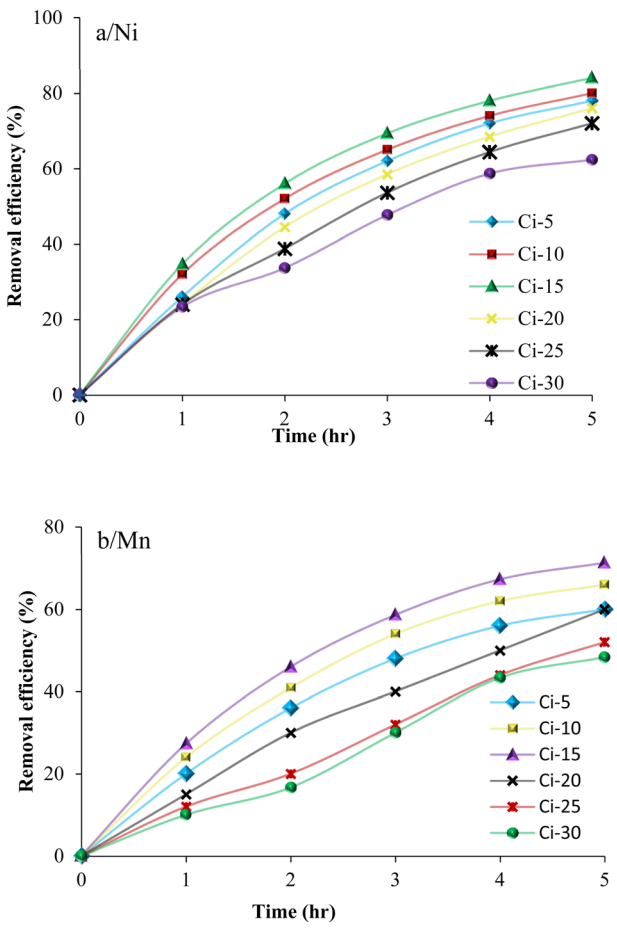


Fig. 14 Effect of the initial concentration on (a) Ni and (b) Mn removal efficiencies.

The $Mn^{2+}$ removal efficiency is influenced by two opposing mechanisms; at an initial concentration of 5 mg $L^{-1}$, the removal efficiency is 60.0%. As the concentration increases to 10 mg $L^{-1}$ and 15 mg $L^{-1}$, the percentage removal efficiency increases to 66.0% and 71.3%, respectively. This elevation is explained by the fact that an increase in the initial concentration leads to a sharp increase in the concentration gradient between the donor solution and the membrane, which is the main driving force of mass transfer. At this point, DEHP is still sufficiently available to bind and transport most of the available Mn ions, allowing for the highest relative efficiency at a concentration of 15 mg $L^{-1}$. After exceeding the optimal concentration (15 mg $L^{-1}$), the percentage removal efficiency begins to decline rapidly to 60%, 52% and 48% at initial concentrations of 20, 25, and 30 mg $L^{-1}$, respectively. This sharp decrease is attributed to the fact that the binding sites on the carrier molecules (DEHP) have reached a state of saturation. In brief, the percentage removal efficiency is affected by two factors: the concentration gradient that increases the efficiency and the saturation of the carrier that limits it. At high concentrations, the saturation effect overwhelms the thrust. The superior removal efficiency of Ni (84%) compared with Mn (71.3%) is mainly due to the difference in the chemical properties of the ions. The DEHP carrier demonstrates a clear advantage in the selection of nickel ions and their ease of transport under the determined operating conditions.[57]

The influence of the initial Ni and Mn concentrations on the acceptor concentration under ideal conditions (pH 6, 60 V, DEHP carrier, and 5-hours contact duration) is illustrated in Fig. 15a and b. Ni demonstrates a distinct direct correlation between its initial concentration and its concentration at the acceptor (Fig. 15a), rising from 0.9 mg $L^{-1}$ at Ci = 5 mg $L^{-1}$ to 4.6 mg $L^{-1}$ at Ci = 30 mg $L^{-1}$. This result specifies that the electrochemical motive force increases with increasing concentration gradient, enabling the production of Ni-DEHP complexes at the donor/membrane contact. An increased concentration of primary Ni enhances mass transfer over the membrane; however, the extraction efficiency may decrease at elevated concentrations due to the saturation of carrier sites.

For $Mn^{2+}$ (Fig. 15b), the acceptor concentration is 1 mg $L^{-1}$ at Ci = 5 mg $L^{-1}$ due to a deficient gradient, which constrains the rate of Mn-DEHP complex formation. At Ci = 10 mg $L^{-1}$, the acceptor concentration increases to 2.9 mg $L^{-1}$, indicating that sufficient ions are present to achieve the semi-saturation of the DEHP binding sites and maximize the transfer rate. However, when the Mn concentration exceeds 10 mg $L^{-1}$, the extraction efficiency decreases due to the saturation of carrier sites within the membrane, coupled with increased resistance to mass transfer resulting from increased viscosity or ion accumulation, which impedes the release of manganese complexes. The receptor solution exhibits a reduction in net extraction despite the elevated driving force.[58]

Fig. 16 shows the relationship between the competitive initial concentration of Mn and Ni ions and current intensity.

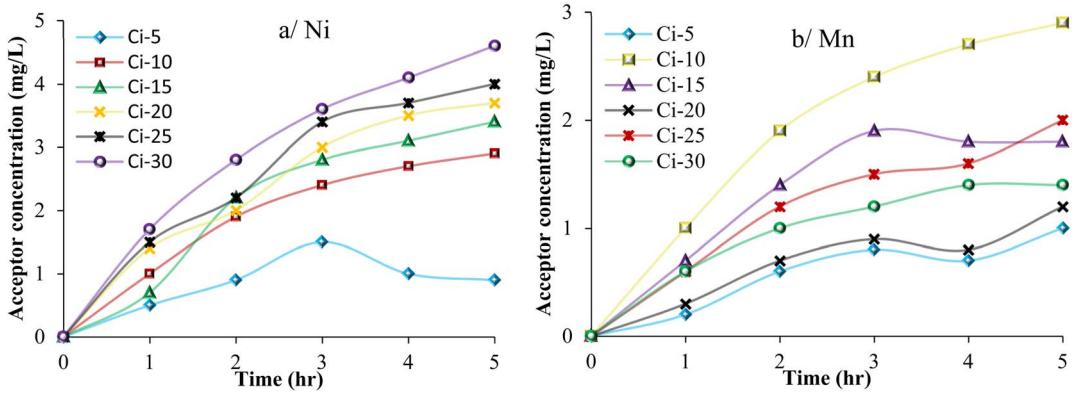


Fig. 15 Effect of the feed concentration on the Ni concentration (a) and Mn concentration (b) at the acceptor.

It's clear that when the competitive initial concentration of Mn and Ni ions increased, current intensity as a result increased at pH 6, 5 hours contact time, and by using the DEHP as a carrier. This is clearly reflected in the recording of the highest Ci-30 concentration to the maximum current value of 68 mA, while the lowest Ci-5 concentration recorded the minimum value of 35 mA. When the availability of reactants increased, the initial concentration of active metal ions $Mn^{2+}$ and $Ni^{2+}$ available per unit volume increased. The higher this concentration, the higher the numerical density of these ions in the solution. These ions are involved in the basic electrochemical reaction, which involves their cross-membrane transport (in the case of an electrochemical cell with a membrane) or their migration towards the electrode for the reduction process. According to the laws of the kinetics of electrochemical reactions, the rate of the reaction on the surface of an electrode (measured as the electric current) is directly proportional to the concentration of the reactant species on the surface of the electrode.[1] An increase in the overall concentration of manganese and nickel in the solution means that more ions can reach the pores of the DEHP carrier and subsequently the surface of the electrode within a certain period of time. This increases the rate of ion consumption. It speeds up the process of electron transfer. The DEHP carrier typically acts as an extraction or transport agent that facilitates the transfer of ions through an organic phase or membrane. Regardless of the carrier's role in speeding up the transport process, the determining factor of the total current remains the initial concentration of the material being transported or reduced. At high concentrations, the number of ions that are "captured" and transported by DEHP is greater, supporting a higher electric current. In summary, it can be said that the total concentration of manganese and nickel is the critical driving force that determines the number of charge carriers available for the reaction and thus directly controls the intensity of the electric current produced.[55]

As shown in Fig. 17, experimental results show that increasing the initial concentration of Mn and Ni ions acts as a major driving force that enhances the flow rate of cations through the supported liquid membrane (SLM). It is clearly observed that the sharp reduction in the donor pH from 6.0 to 1.4 at high concentrations (30 mg $L^{-1}$) is related to the "counter-transport" mechanism, in which protons ($H^+$) migrate rapidly from the acceptor phase to the donor to compensate for the charge deficit caused by the movement of metal cations in the opposite direction under the influence of the electric field. This behavior suggests that an increase in the initial ion load increases the polarization of the membrane, accelerating the

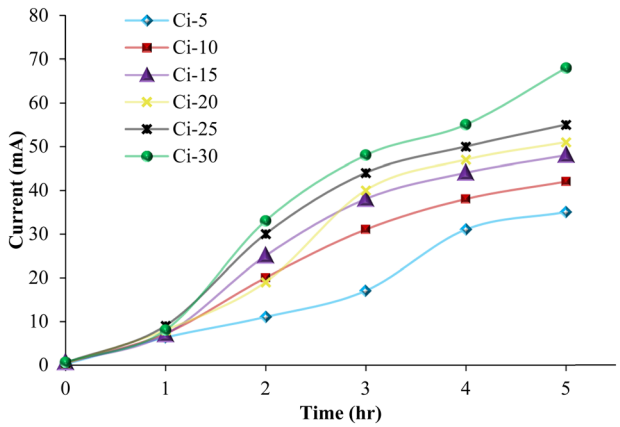


Fig. 16 Effect of the initial concentration on the current density.

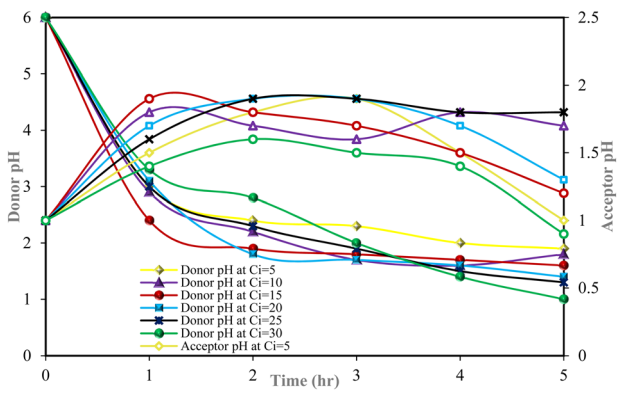


Fig. 17 Influence of the initial concentrations of Mn and Ni on the pH of the donor and the acceptor.

ion exchange dynamics to the state of electrochemical equilibrium. The stability of the acceptor pH at low levels also explains the system's ability to accommodate continuous ion flow, making the EME-SLM method a highly efficient option for the treatment of heavy metal-contaminated water at varying concentrations, where the transfer speed increases with an increase in the initial concentration as a result of the increased chemical voltage gradient across the membrane phase.

## 5. Proposed chemical mechanism

The chemistry in this study can be broken down into three integrated processes as follows.

(1) Complexation chemistry: the carrier used (DEHP) is an organophosphoric acid. At the interface of the aqueous solution and the membrane, an ion exchange reaction and the formation of a chemical complex occur. The suggested chemical equation is as follows:

$$M_{(aq.)}{}^{2+} + 2\overline{(HR)_{2(org.)}} \rightleftharpoons \overline{M(R_2 \cdot HR)_{2(org.)}} + 2H_{(aq.)}{}^{+},$$

where $M^{2+}$ represents the ions of divalent metals ($Ni^{2+}$ or $Mn^{2+}$) in the aqueous phase; $(HR)_2$ represents the carrier (DEHP) in the membrane phase, where it is usually found as a dimer; $M(R_2 \cdot HR)_{2(org)}$ is the metal-carrier complex that travels through the membrane by the electric motive force; and $H^+$ represents the hydrogen ions released into the aqueous solution as a result of ion exchange.

(2) Electrochemical transport: since an electrical voltage (30–60 V) is applied, the electric motive force (electromotive force) accelerates the movement of these charged complexes across the membrane. The electric field directs the complexes towards the cathode (stainless steel), reducing the time required to reach equilibrium compared to passive propagation.

(3) Ionic competition: chemically, nickel and manganese compete for the phosphate groups of DEHP.

(1) $Ni^{2+}$: 84% because its ionic radius and hydration energy increase its familiarity with DEHP in this medium.

(2) $Mn^{2+}$: 71%, the difference is due to the "stability constant" of the complex formed with DEHP.

## 6. Economic feasibility

Although this study was conducted in the batch mode, the proposed EME system shows promising indicators of economic viability. We present a qualitative analysis of the economic feasibility, highlighting the following advantages of the proposed system over traditional methods as follows.

(1) Low energy consumption: the system relies on low voltages (30–60 V) and very low currents, making the operational cost related to electricity lower than that of conventional electrolysis.

(2) Chemical efficiency: the use of the subsidized liquid membrane (SLM) dramatically reduces the amount of the organic carrier (DEHP) required, as the system consumes only micro amounts, significantly reducing the cost of chemicals compared to the "solvent extraction" method.

Table 1 Energy consumption and specific values for removing nickel and manganese metal ions

| Metal | Removal efficiency (%) | Metal removal (g) | Specific energy (kW h $g^{-1}$) |
|---|---|---|---|
| $Ni^{2+}$ | 84 | 0.00084 | 14.3 |
| $Mn^{2+}$ | 73.1 | 0.000731 | 16.4 |

(3) Process intensification: the ability to remove two metals in a single step and in a compact system reduces the capital costs (CAPEX) required to create multiple processing units.

(4) Durability and membrane life: FESEM and AFM assays show the stability of the membrane structure after operation, suggesting that it can be reused for long periods, which is a critical factor in reducing replacement and maintenance costs.

## 7. Energy consumption

In order to determine the suitability and economic feasibility of this technique under real conditions, the total energy consumption was calculated according to the following equation:[59]

$$E = V \times I \times t$$

where $E$ is the energy consumption (W h), $V$ is the voltage (V), $I$ is the current (A), and $t$ is the time (hours).

The calculated energy consumption under optimal conditions (60 V, 5 hours) was 12 W h (or 0.012 kW h). Assuming a solution volume of 100 mL with an initial concentration of 10 mg $L^{-1}$, the total amount of metal in the process system was 1 mg. The result, presented in Table 1, shows that the specific energy for removing nickel (84%) was approximately 14.3 kW h $g^{-1}$, while for removing manganese (73.1%), it was approximately 16.4 kW h $g^{-1}$. The relatively high values are attributed to the small-scale nature of the laboratory experiments and the low initial concentration. Energy efficiency is expected to improve with increased operating volume or higher nutrient concentrations.

## 8. Conclusions

This study concludes that electromembrane extraction (EME) technology represents an efficient and sustainable way to separate heavy metal ions from aqueous solutions, as the results show that the efficiency of the process depends intrinsically on the synergy of chemical and electrical factors. It is shown that increasing the operating time encourages the transition of the mass to the equilibrium state, and the type of organic carrier plays a vital role in the success of the extraction, as the DEHP carrier is proven to be superior to TEHP for the transfer of ions due to its high chemical affinity. On the other hand, the applied voltage is the primary driving force for accelerating the migration of ions across the membrane and

bypassing interstitial resistance, while the pH emerges as a vital factor for regulating performance stability, especially at the intermediate values that ensure the stability of the transported complexes. Morphological tests, such as FESEM and AFM analyses, support these conclusions, as changes in the surface roughness and pore fullness confirm successful organic carrier stabilization and ion exchange effectiveness, making this technology a promising choice for industrial water treatment processes. Although this study shows high efficiency at the batch-experiment laboratory scale, further research is needed to assess the membrane's stability over the long term in continuous industrial operations.

## Conflicts of interest

The authors declare that they have no known competing financial interests or personal relationships that could have appeared to influence the work reported in this paper.

## Data availability

All data related to the paper will be made available upon request.

## References

1 V. Coman, B. Robotin and P. Ilea, Nickel recovery/removal from industrial wastes: A review, *Resour. Conserv. Recycl.*, 2013, **73**, 229–238.
2 B. Swain, K. Sarangi and R. P. Das, Effect of different anions on separation of copper and zinc by supported liquid membrane using TOPS-99 as mobile carrier, *J. Membr. Sci.*, 2004, **243**, 189–194.
3 T. J. Al-Musawi, F. A. Alnasrawi, S. L. Kareem and A. A. Mohammed, Simultaneous adsorption of cadmium, zinc, and lead ions from aqueous solution by Montmorillonite clay coated with MgCuAl-LDH nanoparticles, *J. Indian Chem. Soc.*, 2024, **101**, 101378.
4 A. M. Ahmed and S. L. Kareem, Comprehensive Review of Arundo donax and Lemna gibba for Phytoremediation Efficacy in Sustainable Wastewater Treatment, *Environ. Claims J.*, 2025, **37**, 601–627.
5 S. K. Mondal, M. K. Beriya and P. Saha, Separation and Recovery of Nickel and Zinc from Synthetic Wastewater Using Supported Liquid Membranes with in Situ Electrodeposition, *Ind. Eng. Chem. Res.*, 2019, **58**, 9970–9987.
6 J. Baby, J. S. Raj, E. T. Biby, P. Sankarganesh, M. V. Jeevitha, S. U. Ajisha and S. S. Rajan, Toxic effect of heavy metals on aquatic environment, *Int. J. Biol. Chem. Sci.*, 2010, **4**(4), 939–952.
7 A. M. Ahmed and S. L. Kareem, Evaluating the role of hydraulic retention time (HRT) in pollutant removal efficiency using Arundo donax in vertical subsurface flow constructed wetlands, *Biorem. J.*, 2024, 1–15.
8 D. N. Ahmed, M. A. Hussein, M. B. Abdul-Kareem, W. H. Hassan, N. Al-Ansari and A. A. H. Faisal, Green Synthesis of Hybrid Iron Oxides/Graphene Immobilization on the Iron Slag for Reclamation Congo Red Dye-Water, Water, Air, *Soil Pollut.*, 2023, **234**, 778.
9 S. A. Hardan and S. K. Ali, Adsorption of methylene blue from aqueous solution by orange peel gel, *AIP Conf. Proc.*, 2024, **3009**, 030093.
10 S. A. Hardan and S. K. Ali, A comparison between banana peel powder and gel for removing methylene blue dye from aqueous solution, *AIP Conf*, *Proc.*, 2024, **3009**, 030087.
11 D. N. Ahmed and M. A. Hussein, Sustainable Synthesis and Immobilization of Mg/Fe-LDH-Functionalized Biochar Derived From Spinach Waste in Sodium Alginate for the Effective Elimination of Tetracycline and Cadmium, *Remed. J.*, 2026, **36**, e70055.
12 M. A. Hussein, D. N. Ahmed, A. S. Kadhim and S. L. Kareem, Effective W/O emulsion performance to extract the antibiotic co-trimoxazole from wastewater, *Desalination Water Treat.*, 2023, **282**, 2237–2245.
13 A. D. Albdiri, A. A. Mohammed, M. Hussein and S. Koter, Modeling of lead ions transport through a bulk liquid membrane, *Desalination Water Treat.*, 2020, **181**, 213–220.
14 M. Shuwaili, M. A. Hussein, S. A. Hardan and K. Al-Khafaji, Experimental processing and quantum mechanical insights using surface modification of Nano-Fe3O4@Oleic acid for the removal of phenol, *J. Indian Chem. Soc.*, 2026, **103**, 102511.
15 E. Y. Salih, Y. J. Jameel, A. W. Saeed, M. A. H. Al-Beayaty, M. D. Salman, M. A. Hussein, Performance evaluation of p-NiO/n-FTO heterojunction UV photodetector, In *IOP Conference Series: Earth and Environmental Science*, IOP Publishing, 2025, vol. 1493(1), p. 012017.
16 M. A. Hussein, H. A. Shamkhi, Z. N. Abd and F. H. Abbas, Experimental study of chemical oxygen demand removal by electrochemical oxidation treatment of petroleum refinery wastewater by using response surface methodology, *Desalination Water Treat.*, 2023, **316**, 371–382.
17 G. Chen, Electrochemical technologies in wastewater treatment, *Sep. Purif. Technol.*, 2004, **38**, 11–41.
18 M. A. Malik, M. A. Hashim and F. Nabi, Ionic liquids in supported liquid membrane technology, *Chem. Eng. J.*, 2011, **171**, 242–254.
19 M. A. Hussein and D. N. Ahmed, Efficient nano emulsion Co-stabilized by iron nano oxides coated with graphene slag for removal of Co-trimoxazole, *J. Indian Chem. Soc.*, 2025, **102**, 101538.
20 P. K. Parhi and K. Sarangi, Separation of copper, zinc, cobalt and nickel ions by supported liquid membrane technique using LIX 84I, TOPS-99 and Cyanex 272, *Sep. Purif. Technol.*, 2008, **59**, 169–174.
21 H. Duan, Z. Wang, X. Yuan, S. Wang, H. Guo and X. Yang, A novel sandwich supported liquid membrane system for simultaneous separation of copper, nickel and cobalt in ammoniacal solution, *Sep. Purif. Technol.*, 2017, **173**, 323–329.
22 H. Ma, O. Kökkılıç, R. Langlois, X. Song, Y. Qin and K. E. Waters, Selective separation of copper and nickel ions from aqueous solutions containing calcium by

emulsion liquid membranes using central composite design, *Can. J. Chem. Eng.*, 2019, **97**, 1881–1893.

23 R. N. Raja Sulaiman, N. Othman, N. F. Mohamed Noah and N. Jusoh, Removal of nickel from industrial effluent using a synergistic mixtures of acidic and solvating carriers in palm oil-based diluent via supported liquid membrane process, *Chem. Eng. Res. Des.*, 2018, **137**, 360–375.

24 L. Chimuka, E. Cukrowska, M. Michel and B. Buszewski, Advances in sample preparation using membrane-based liquid-phase microextraction techniques, *TrAC, Trends Anal. Chem.*, 2011, **30**, 1781–1792.

25 N. R. Kadhim, H. M. Flayeh and A. H. Abbar, Exploring electromembrane extraction and liquid membrane for efficient removal of heavy metals from aqueous solutions: An overview, *Environ. Eng. Res.*, 2024, **29**(3), 230463.

26 K. F. Seip, M. Faizi, C. Vergel, A. Gjelstad and S. Pedersen-Bjergaard, Stability and efficiency of supported liquid membranes in electromembrane extraction—a link to solvent properties, *Anal. Bioanal. Chem.*, 2014, **406**, 2151–2161.

27 S. K. Singh, S. K. Misra, S. C. Tripathi and D. K. Singh, Studies on permeation of uranium (VI) from phosphoric acid medium through supported liquid membrane comprising a binary mixture of PC88A and Cyanex 923 in n-dodecane as carrier, *Desalination*, 2010, **250**, 19–25.

28 W. Zhang, C. Cui and Z. Hao, Transport Study of Cu(II) Through Hollow Fiber Supported Liquid Membrane, *Chin. J. Chem. Eng.*, 2010, **18**, 48–54.

29 B. K. Dutta, Principles of mass transfer and separation processes, *J. Chem. Eng.*, 2009, **87**, 818–819.

30 C. Román-Hidalgo, L. Barreiros, M. Villar-Navarro, G. López-Pérez, M. J. Martín-Valero and M. A. Segundo, Electromembrane extraction based on biodegradable materials: Biopolymers as sustainable alternatives to plastics, *TrAC, Trends Anal. Chem.*, 2023, **162**, 117048.

31 P. Kubáň and P. Boček, Micro-electromembrane extraction across free liquid membranes. Instrumentation and basic principles, *J. Chromatogr. A*, 2014, **1346**, 25–33.

32 D. Fuchs, C. R. Hidalgo, M. Ramos Payán, N. J. Petersen, H. Jensen, J. P. Kutter and S. Pedersen-Bjergaard, Continuous electromembrane extraction coupled with mass spectrometry – Perspectives and challenges, *Anal. Chim. Acta*, 2018, **999**, 27–36.

33 N. R. Kadhim, A. H. Abbar and H. M. Flayeh, Removal of copper from a simulated wastewater by electromembrane extraction technique using a novel electrolytic cell provided with a flat polypropylene membrane infused with 1-octanol and DEHP as a carrier, *Case Stud. Chem. Environ. Eng.*, 2023, **8**, 100430.

34 M. Khayet, Characterization Of Membrane Distillation Membranes By Tapping Mode Atomic Force Microscopy, in *Recent Advances in Multidisciplinary Applied Physics*, ed. A. Méndez-Vilas, Elsevier Science Ltd, Oxford, 2005, pp. 141–148.

35 Z. Xu, Z. Liu, P. Song and C. Xiao, Fabrication of super-hydrophobic polypropylene hollow fiber membrane and its application in membrane distillation, *Desalination*, 2017, **414**, 10–17.

36 P. Amirabedi, A. Akbari, R. Yegani and S. Raveshiyan, CO2 Stripping from Monoethanolamine through a Polypropylene/CH3SiO2 Composite Hollow-Fiber Membrane Contactor, *Chem. Eng. Technol.*, 2022, **45**, 1512–1521.

37 R. W. Al-Khateeb, A. A. Mohammed, M. A. Hussein and N. A. Mohammed, Synthesis of green nanoparticles as stabilizing agents in nano-emulsion for phenol removal from wastewater, *J. Mol. Liq.*, 2025, **420**, 126838.

38 R. Ramezani, L. Di Felice and F. Gallucci, A Review on Hollow Fiber Membrane Contactors for Carbon Capture: Recent Advances and Future Challenges, *Processes*, 2022, **10**(10), 2103.

39 M. Fukuda, Y. Nishite, E. Murata, K. Namekawa, T. Mori, T. Tanaka and K. Sakai, Determining Accurate Pore Structures of Polypropylene Membrane for ECMO Using FE-SEM Under Optimized Conditions, *Membranes*, 2025, **15**(6), 174.

40 R. O. Martins, G. L. de Araújo, R. C. Simas and A. R. Chaves, Electromembrane extraction (EME): Fundamentals and applications, *Talanta Open*, 2023, **7**, 100200.

41 M. Á. Bello-López, M. Ramos-Payán, J. A. Ocaña-González, R. Fernández-Torres and M. Callejón-Mochón, Analytical Applications of Hollow Fiber Liquid Phase Microextraction (HF-LPME): A Review, *Anal. Lett.*, 2012, **45**, 804–830.

42 F. Gholami, A. Asadi and A. A. Zinatizadeh, Efficient heavy metals and salts rejection using a novel modified polysulfone nanofiltration membrane, *Appl. Water Sci.*, 2022, **12**, 146.

43 G. Moradi, R. Heydari, S. Zinadini, M. Rahimi and F. Gholami, High-performance nanofiltration membranes consisting of the new functionalized mesoporous for enhanced antifouling attributes and simultaneous removal of salts, dyes and heavy metals, *Environ. Technol. Innovat.*, 2021, **24**, 101929.

44 K. Mubeena and G. Muthuraman, Solvent extraction technique for removal and recovery of nickel from effluent by Tri methyl amine as a carrier, Mubeena, *Int. J. Comput. Sci. Eng. Inf. Technol. Res.*, 2015, **4**, 128–137.

45 M. Amini, A. Rahbar-Kelishami, M. Alipour and O. Vahidi, Supported liquid membrane in metal ion separation: An overview, *J. Membr. Sci. Res.*, 2018, 121–135.

46 M. Monesi, M. Khatibi and A. Rahbar-Kelishami, A simulation study of an electro-membrane extraction for enhancement of the ion transport via tailoring the electrostatic properties, *Sci. Rep.*, 2022, **12**(1), 12170.

47 H. Pei, C. Xiao, L. Xing and Z. Tu, Self-Water-Removal and Voltage Behavior Improvement of Dead-Ended Proton Exchange Membrane Fuel Cell Stack at Steady-State and Dynamic Conditions, *Front. Energy Res.*, 2022, **10**, 902829.

48 A. Timmaoui, M. Ferhat, N. S. Ferhat and A. Hamdi, Understanding ammonia's role in mitigating concentration polarization in anion-exchange membrane electrodialysis, *Turk. J. Chem.*, 2024, **48**, 843–855.

49 G. Zhu, Y. Wang, Q. Huang, R. Zhang, D. Chen, S. Wang and X. Yang, Emulsion liquid membrane for simultaneous extraction and separation of copper from nickel in ammoniacal solutions, *Miner. Eng.*, 2022, **188**, 107849.
50 K. Sarangi and R. P. Das, Separation of copper and zinc by supported liquid membrane using TOPS-99 as mobile carrier, *Hydrometallurgy*, 2004, **71**, 335–342.
51 A. Gjelstad, T. M. Andersen, K. E. Rasmussen and S. Pedersen-Bjergaard, Microextraction across supported liquid membranes forced by pH gradients and electrical fields, *J. Chromatogr. A*, 2007, **1157**, 38–45.
52 N. Aranda-Merino, C. Román-Hidalgo, J. L. Pérez-Bernal, M. Callejón-Mochón, M. Villar-Navarro and R. Fernández-Torres, Effect of Aliquat®336 on supported liquid membrane on electromembrane extraction of non-steroidal anti-inflammatory drugs, *Microchem. J.*, 2021, **168**, 106459.
53 G. Alvial-Hein, H. Mahandra and A. Ghahreman, Separation and recovery of cobalt and nickel from end of life products via solvent extraction technique: A review, *J. Clean. Prod.*, 2021, **297**, 126592.
54 M. Farah, J. Giralt, F. Stüber, J. Font, A. Fabregat and A. Fortuny, Supported liquid membranes for the removal of pharmaceuticals from aqueous solutions, *J. Water Proc. Eng.*, 2022, **49**, 103170.
55 N. R. Kadhim, H. M. Flayeh and A. H. Abbar, Electromembrane extraction of Cadmium (II) using a novel design of electrochemical cell with a flat sheet supported liquid membrane, *Process Saf. Environ. Prot.*, 2025, **197**, 107035.
56 M. Lech, O. Gala, K. Helińska, K. Kołodzińska, H. Konczak, Ł. Mroczyński and E. Siarka, Membrane Separation in the Nickel-Contaminated Wastewater Treatment, *Waste*, 2023, **1**, 482–496.
57 M. Ramos-Payán, R. Fernández-Torres, J. L. Pérez-Bernal, M. Callejón-Mochón and M. Á. Bello-López, A novel approach for electromembrane extraction based on the use of silver nanometallic-decorated hollow fibers, *Anal. Chim. Acta*, 2014, **849**, 7–11.
58 P. K. Parhi, Supported liquid membrane principle and its practices: A short review, *J. Chem.*, 2013, **2013**(1), 618236.
59 A. J. Bard, L. R. Faulkner, *Electrochemical Methods: Fundamentals and Applications*, 2nd edn, Wiley, 2001.